Metric Engineering of Soft Molecular Host Frameworks

K. TRAVIS HOLMAN, ADAM M. PIVOVAR, JENNIFER A. SWIFT, AND MICHAEL D. WARD*

Department of Chemical Engineering and Materials Science, University of Minnesota, Minneapolis, Minnesota 55455

Received July 5, 2000

ABSTRACT

The self-assembly and solid-state structures of host−guest inclusion compounds with lamellar architectures based on a common building block, a resilient hydrogen-bonded sheet consisting of guanidinium ions and sulfonate moieties of organodisulfonate "pillars", are described. The pillars connect adjacent sheets to generate galleries with molecular-scale cavities occupied by guest molecules. The size, shape, and physicochemical character of the inclusion cavities can be systematically adjusted by interchanging framework components while maintaining the lamellar architecture, enabling prediction and control of crystal lattice metrics with a precision that is unusual for "crystal engineering". The reliability of the lamellar architecture is a direct consequence of conformational flexibility exhibited by these hosts that, unlike rigid systems, enables them to achieve optimal packing with guest molecules. The adaptability of these hosts is further reflected by an architectural isomerism that is driven by guest templating during assembly of the inclusion compounds. Host frameworks constructed with various pillars display metric interdependences among specific structural features that reveal a common mechanism by which these soft frameworks adapt to different guests. This unique feature facilitates structure prediction and provides guidance for the design of inclusion compounds based on these hosts.

Introduction

A broad range of scientific endeavors has, especially in recent years, established a growing interest in the molecule-based approach toward the development of future technologies. "Soft" materials based on molecular components—e.g., block copolymers, organic thin films, molecular crystals—promise precision engineering of specific properties and functions since their synthesis is inherently modular. That is, in principle, molecular subunits or building blocks, whose exact structure and function may be manipulated using the tools of synthetic chemistry, can be combined in a rational manner, using appropriate strategies, to design solid-state structure. Unfortunately, structural control in molecular materials is often frustrated by the delicate, noncovalent nature of the intermolecular interactions that govern solid-state assembly. This problem is readily apparent from numerous investigations wherein "crystal engineering",[1] a discipline devoted to guiding the assembly of molecules into desirable crystalline architectures, is thwarted by an inability to maintain structural control when making even the slightest changes in the structures of the molecular components. Crystal engineering can be even more challenging when synthesizing materials consisting of two or more molecular components. Though the hybrid nature of such materials can expand the range of achievable properties, multiple components add complexity with respect to the number of possible compositions and structural permutations. Design strategies therefore require predictable assembly, preferably through the use of molecular or supramolecular "modules" that organize through specific intermolecular interactions.

Since the initial discoveries and structure determinations of the earliest inclusion compounds,[2] a great deal of effort has been directed toward the design of low-density host frameworks capable of including molecular guests. The demonstration of porosity,[3] magnetic behavior,[4] ferroelasticity,[5] nonlinear optical effects,[6] chemical storage,[7] and catalysis[8] has established the significance of inclusion compounds for materials applications. Moreover, inclusion compounds are inherently versatile with respect to materials design because they allow crystal architecture, furnished by the host framework, to be separated from function, which suitable guests may introduce. While numerous investigations of inclusion compounds based on a variety of organic hosts such as thiourea, tri-*o*-thymotide, perhydrotriphenylene, choleic acid, and cyclotriveratrylene have advanced the understanding of inclusion phenomena, most hosts cannot be chemically modified without destroying the basic crystal architecture required for guest inclusion. This prevents systematic modification of the inclusion cavities and limits the potential of such hosts.

In this Account we describe a family of designer host frameworks, developed in our laboratory, that is based on a robust, layered (i.e., lamellar), hydrogen-bonded structural motif. The hydrogen-bonded layers are separated in

* To whom correspondence should be addressed.

K. Travis Holman received his B.S. degree in chemistry and mathematics from St. Mary's University, Halifax, in 1994, and his Ph.D. in chemistry with J. L. Atwood at the University of Missouri in 1998. He is currently a Natural Sciences and Engineering Research Council of Canada postdoctoral research fellow at the University of Minnesota.

Adam M. Pivovar received his B.S. degree in chemical engineering from the University of Wisconsin in 1995, and is currently a graduate student in the chemical engineering program at the University of Minnesota. He will join the staff of the National Institute of Standards and Technology (Gaithersburg, MD) in the fall of 2000 as a National Research Council Postdoctoral Fellow.

Jennifer A. Swift received her B.A. degree in chemistry from Bowdoin College in 1991, and her Ph.D. in chemistry with J. M. McBride at Yale University in 1997. After postdoctoral research at the University of Minnesota, she joined the Department of Chemistry at Georgetown University as Clare Boothe Luce Assistant Professor of Chemistry.

Michael D. Ward received his B.S. degree in chemistry from the William Paterson College of New Jersey in 1977, and his Ph.D. degree with J. Schwartz at Princeton University in 1981. He was a Welch postdoctoral fellow with A. J. Bard at the University of Texas, Austin, between 1981 and 1982. He joined the research staff at Standard Oil of Ohio in Cleveland in 1982. In 1984, he became a member of the research staff at the Dupont Central Research and Development Laboratories. He joined the faculty of the Department of Chemical Engineering and Materials Science at the University of Minnesota in 1990, where he is currently a Distinguished McKnight University Professor and director of the University of Minnesota Materials Research Science and Engineering Center.

10.1021/ar970272f CCC: $20.00 © 2001 American Chemical Society
Published on Web 11/17/2000

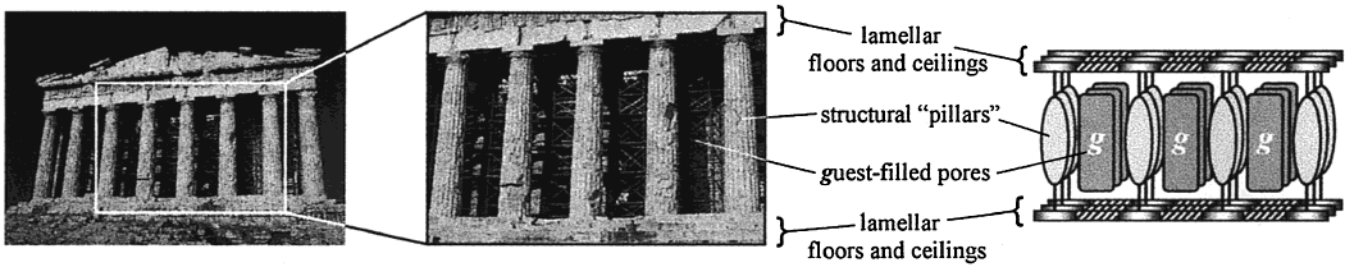

FIGURE 1. The Parthenon, here filled with some construction material, bears a remarkable resemblance to one type of crystal architecture observed in the inclusion compounds described in this Account.

the third dimension by molecular "pillars", thereby creating a three-dimensional framework with inclusion cavities between the layers. The pillar heights can be adjusted through organic synthesis so that the size, shape, and chemical functionality of the inclusion cavities can be modified systematically like an architect would modify the specifications of a building. Indeed, the structures of these compounds resemble the architectures of simple buildings, wherein the hydrogen-bonded layers mimic floors and ceilings and the molecular pillars mimic walls or columns (Figure 1). Of course, any building is designed to have empty space that can be occupied by animate or inanimate objects. The host frameworks described here are similar in this respect, though the occupants (i.e., guest molecules) are required for structural stability. The guests, however, can be removed by demolishing the host framework (i.e., dissolving) and rebuilding (i.e., crystallizing) with different guests. Another feature of these host frameworks, not shared by cementitious structures, is an inherent softness that allows them to conform to differently sized and shaped guest molecules.

Though we are exploring applications for these materials (see Epilogue), we intend here to illustrate how crystal engineering can be extended beyond the control of global structure characteristics such as dimensionality and topology. That is, we illustrate that specific *metric* parameters (e.g., intermolecular contact distances, lattice dimensions, angles) can be predicted and interdependencies between key structural parameters can be described quantitatively in a manner that embodies true engineering principles.[9−11] This is made possible by the persistence of the aforementioned two-dimensional hydrogen-bonded motif in over 200 structures, facilitating systematic comparisons and meticulous analysis of structural metrics to a degree that is rare in crystal engineering. The metric interdependencies for the compounds discussed here reveal well-behaved mechanisms for conformational adaptation of the host framework to differently sized and shaped guests. Elucidation of these mechanisms provides a basis for designing new inclusion compounds with various host−guest combinations and manipulating key structural features with unprecedented precision, features that are crucial to the advancement of crystal engineering.

Design Concepts for Inclusion Hosts

Over the past several years, our laboratory has demonstrated that guanidinium ions (**G**, $C(NH_2)_3^+$) and various organodisulfonates ($^-O_3S-R-SO_3^-$) assemble, in the presence of suitable guest molecules, into crystalline host frameworks with exceptionally reproducible lamellar architectures. The syntheses of these materials were actually prompted by our earlier studies of guanidinium organo-*mono*sulfonate salts,[12−14] which possess architectures that are homologous with the organodisulfonate structures. Though this Account focuses on the organodisulfonate materials, the crystal engineering principles described here have evolved from our studies of both classes of compounds.

The basic building block of these host frameworks is a two-dimensional (2-D) sheet of **G** ions and sulfonate (**S**) groups, the latter belonging to an organodisulfonate that serves as a pillar connecting two adjacent **GS** sheets. These sheets typically exhibit a "quasihexagonal" motif that stems from ionically assisted, intermolecular (**G**)N−H···O(**S**) H bonds between an equivalent number (six) of **G** protons and H-bonding acceptor sites on the sulfonate oxygen atoms of complementary D_{3h} **G** ions and the C_{3v} sulfonate moieties (Figure 2). Though formation of these sheets can be perturbed when the organic portion of the sulfonate contains a functional group that competes for hydrogen bonding with the **G** ions or **S** moieties, the robustness of the quasihexagonal motif, and a closely related "shifted-ribbon" motif (vide infra), is evidenced by their ubiquitous occurrence.

The quasihexagonal **GS** sheet can be described as 1-D **GS** "ribbons" fused along the ribbon edges by lateral (**G**)N−H···O(**S**) H bonds. The repeat distances along the **GS** ribbon direction fall into a narrow range ($a_1 = 7.5 \pm 0.2$ Å), reflecting relatively stiff H bonds within the ribbon. The examples that follow illustrate that the lateral (**G**)N−H···O(**S**) H-bonds serve as flexible "hinges" that permit puckering of the **GS** sheet without an appreciable change in the near-linear geometries of the H bonds. The *inter-ribbon puckering angle* (θ_{IR}), which for convenience and measurement consistency we determine from the centroid of two sulfur atoms on a selected **GS** ribbon and the nearest sulfur atoms on the two adjacent ribbons,[15] dictates the repeat distance normal to the ribbon direction (b_1). The observed values of b_1 range from 13.0 Å (twice the width, w, of a **GS** ribbon) for a perfectly flat sheet to as little as 7.3 Å for a highly puckered sheet, which still retains the quasihexagonal motif. Importantly, the dense packing of atoms within the **GS** sheet precludes self-

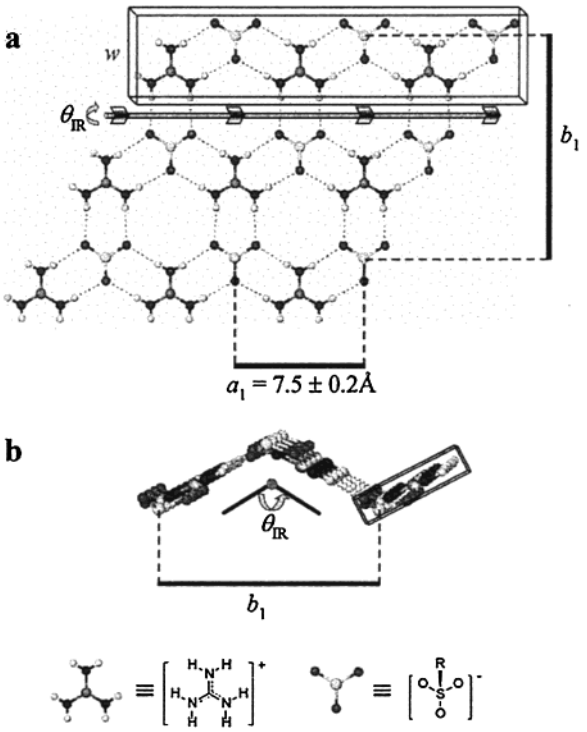

FIGURE 2. (a) Model of a guanidinium−sulfonate (**GS**) sheet. The box highlights a single **GS** ribbon, which contains the lattice dimension a_1 and has a fixed width of $w = a_1 \sin(60°) = 6.5$ Å for an ideal sheet. The **GS** sheet can pucker about a flexible hinge defined by hydrogen bonds between the ribbons. This puckering, defined by θ_{IR}, shortens b_1, the lattice constant perpendicular to the ribbons. (b) A puckered **GS** sheet as viewed along the ribbon direction.

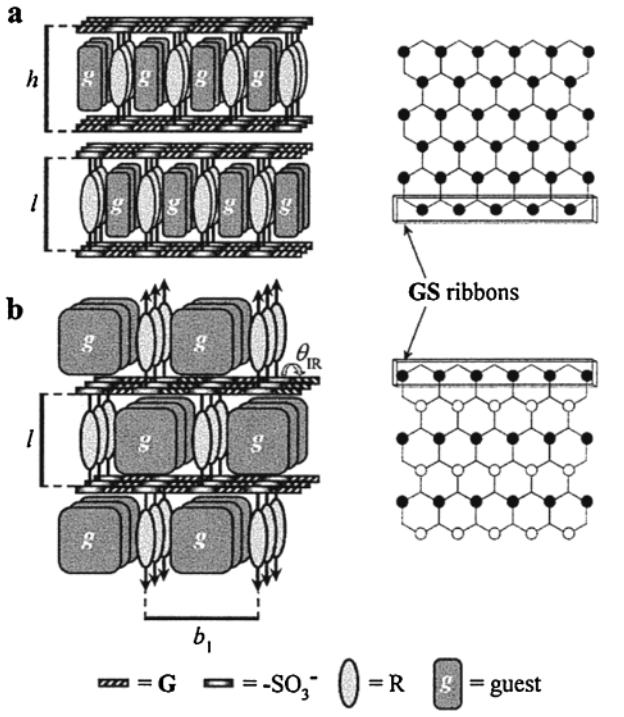

FIGURE 3. Schematic representations of **GS** host frameworks with the (a) pillared discrete bilayer and (b) pillared continuous "simple-brick" architectures. The panels at the left depict views edge-on to the **GS** sheet, whereas the panels at the right schematically code the up/down pillar orientation on each sheet, represented as hexagons, in the respective architectures (up = filled circles, down = open circles).

interpenetration of these networks, which often frustrates the formation of open framework structures.[16]

The two-dimensional character of the **GS** sheet promotes the formation of lamellar crystalline architectures. We also surmise that lamellar architectures are favored by the tendency of the polar (**GS** sheets) and nonpolar (organic residues) regions to segregate, in a manner similar to lamellar surfactant and block copolymer microstructures. The organic groups appended to the sulfonates serve as pillars to build the lattice in the third dimension and introduce tunable chemical functionality to the resulting lattice. The simplest architecture is one we describe as a "pillared discrete bilayer", in which two adjacent **GS** sheets are connected by organodisulfonate pillars that span galleries between the sheets (Figure 3). Stacking of these bilayers generates the complete 3-D crystal structure. The metrics of the **GS** sheet, specifically the sulfonate−sulfonate spacing, prevent the pillars from achieving close packing in the galleries. This generally affords inclusion cavities that are occupied by guest molecules during assembly of the lattice. We note that these cavities are "virtual" as they do not exist in the absence of the guests.

The discrete bilayer architecture requires that all the organodisulfonate pillars project from only one side, either all up or all down, of each **GS** sheet. It is readily apparent that other pillar topologies, described by the "up/down" projection of the pillars from each **GS** sheet, are feasible. For example, we have synthesized numerous **GS** inclusion compounds with a "simple brick" architecture, wherein the pillars project from the same side of each **GS** *ribbon* but alternate their up/down orientation on adjacent ribbons. The **GS** sheets in this form are connected continuously along the third dimension, and the inclusion cavity volume is nominally twice that of the corresponding bilayer, thereby enabling inclusion of larger guest molecules. If the *supramolecular* connectivity (e.g., the quasi-hexagonal **GS** sheet) is identical for bilayer and simple brick hosts having the same pillar, the frameworks can be regarded as *architectural isomers* that differ only with respect to the topological arrangement of the building blocks.[17] It should be noted that, in principle, an infinite number of bricklike frameworks with different up/down pillar arrangements are possible, each producing uniquely sized and shaped inclusion cavities.

Metric Control with Pillar Libraries

The volumes, heights, shapes, and chemical environments of the inclusion cavities, created in the gallery regions between adjacent **GS** sheets, can be manipulated by the choice of organodisulfonate pillar. The general ease with which many simple organodisulfonates can be synthesized has enabled us to create a diverse library of pillars that affords a substantial set of inclusion compounds in which inclusion cavity metrics and characteristics can be sys-

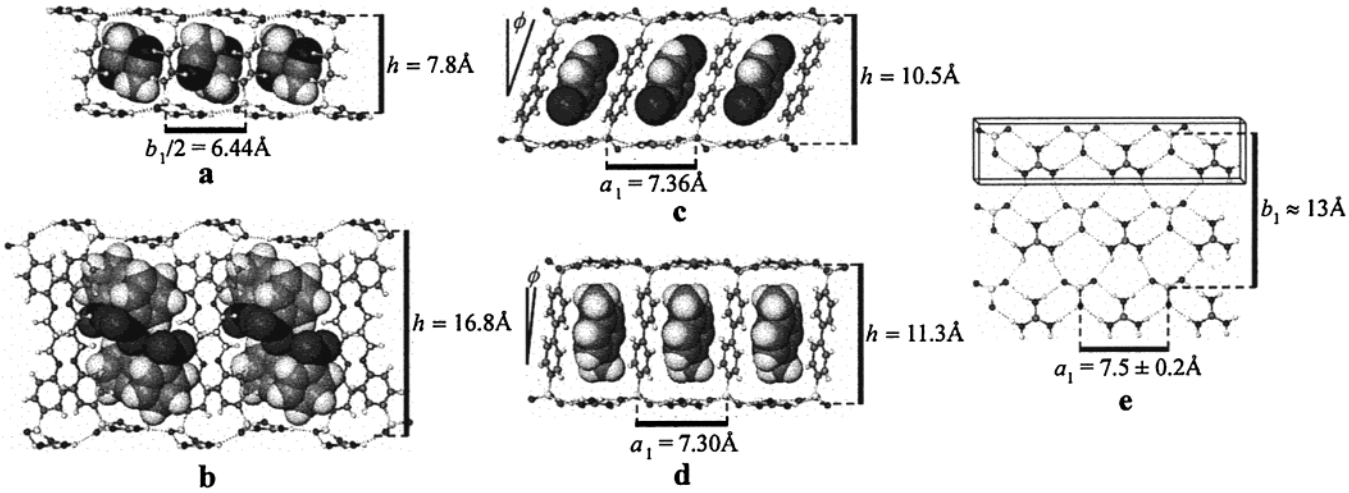

FIGURE 4. Crystal structures of bilayer inclusion compounds (a) **G$_2$BuDS**·2(CH_3CN), (b) **G$_2$BSPP**·2($C_6H_5NO_2$), (c) **G$_2$BPDS**·(*p*-dichlorobenzene), and (d) **G$_2$BPDS**·(*p*-xylene). (e) The "shifted-ribbon" **GS** sheet motif observed in some **GS** bilayer frameworks.

Scheme 1

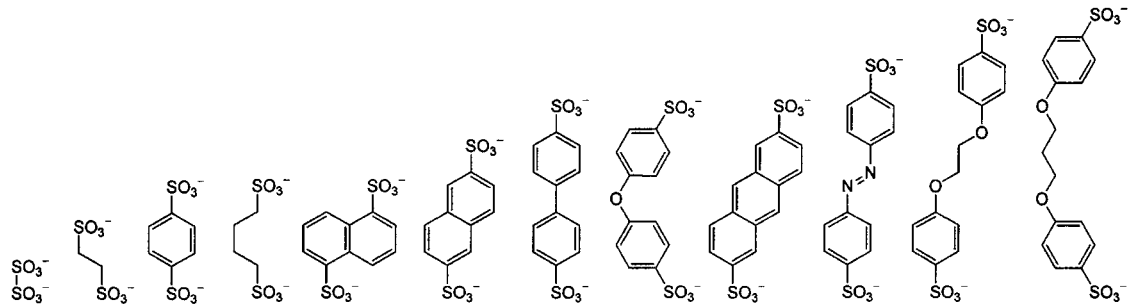

tematically adjusted.[18−20] Scheme 1 illustrates some of these pillars, with lengths ranging from l = 2.1 Å to 15.6 Å, where l is the intramolecular S···S separation [**DT** = dithionate; **EDS** = 1,2-ethanedisulfonate; **BDS** = 1,4-benzenedisulfonate; **BuDS** = 1,4-butanedisulfonate; **1,-5NDS** = 1,5-naphthalenedisulfonate; **2,6NDS** = 2,6-naphthalenedisulfonate; **BPDS** = 4,4′-biphenyldisulfonate; **PEDS** = 4,4′-phenyletherdisulfonate; **ADS** = 2,6-anthracenedisulfonate; **ABDS** = 4,4′-azobenzenedisulfonate; **BSPE** = 1,2-bis(*p*-sulfophenoxy)ethane; **BSPP** = 1,3-bis-(*p*-sulfophenoxy)propane)].

With the exception of **DT** and **EDS**, which are too short to produce inclusion cavities of sufficient size for guest inclusion, **G** salts of the pillars in Scheme 1 form crystalline inclusion compounds in the presence of appropriate guests. We have now synthesized nearly 200 **GS** inclusion compounds that crystallize as either bilayer or continuous brick host architectures, depending on the individual characteristics of the pillar and/or included guest. The guest molecules range from small solvent molecules (e.g., acetone, acetonitrile, etc.) to moderately long linear guests (e.g., alkenes/alkynes, nitriles) to large aromatic molecules (e.g., anthracene, pyrene). These inclusion compounds are crystallized by conventional methods from an aqueous or alcohol solution of the guest-free **GS** apohost and a selected guest. This large database of structural information, based on a systematic study of closely related compounds, has proved valuable for advancing general crystal engineering principles.

Bilayer Host Architectures

To a first approximation, the gallery heights (h) of the bilayer host architectures, as defined by the shortest distance between the mean planes of the adjacent **GS** sheets, can be increased systematically by simply increasing the pillar length (l). This is accompanied by a corresponding increase in the overall volume of the inclusion cavities (V_{inc}) and, therefore, an increased size and/or number of included guest molecules. This is evident from a comparison of **G$_2$BuDS**·2(acetonitrile) (h = 7.8 Å) and **G$_2$BSPP**·2(nitrobenzene) (h = 16.8 Å) (Figure 4a,b). The gallery heights cannot always be surmised directly from the pillar length alone because the bilayer host frameworks are not completely rigid. A systematic investigation of over 30 bilayer inclusion compounds with the composition **G$_2$BPDS**·n(guest) revealed that these frameworks are somewhat flexible, enabling them to "shrink-wrap" about slightly undersized guests to achieve dense packing and optimized host−guest interactions.[20] Subsequent studies

of frameworks with other pillars have revealed that the measured values of V_{host}, the unit volume occupied by a given host (framework only), is essentially independent of the guest (e.g., $V_{host} = 335 \pm 3$ Å^3 for **G$_2$BPDS**),[21] indicating that the shrink-wrapping principally involves conformational changes of the host rather than shortening of the H bond lengths. This conformational softness stems from one or more contributions, including (i) a slight buckling of the **GS** *bilayer* sheet, (ii) conformational freedom associated with the molecular pillar, including turnstile rotation of the pillars about the C−S bonds or, as in the case of **BPDS**, internal conformation flexibility, (iii) tilting of the pillars with respect to the mean plane of the **GS** sheets (defined by a tilt angle ϕ between the pillar axis and a normal to the **GS** sheets), and (iv) the formation of a "shifted-ribbon" **GS** sheet motif (Figure 4e) in which adjacent connected ribbons are shifted from the quasi-hexagonal arrangement, by as much as $a_1/2$, such that they are connected by one strong (**G**)N−H···O(**S**) H bond (d_O···H ≈ 2.0 Å) and one weaker one (d_O···H ≈ 2.5 Å). The shifted ribbon motif is unique to the bilayer framework.

Arene-based pillars in the bilayer framework form densely packed walls flanking one-dimensional channels within the gallery regions. The arene planes typically are nearly *parallel* to the **GS** ribbons for bilayer frameworks with the quasihexagonal **GS** sheet. The guest filled channels coincide with a_1, parallel to the ribbon direction. Consequently, the width of these channels is $b_1/2$ (ranging from 6.2 to 6.5 Å) minus the van der Waals thickness of the pillars. In contrast, the pillars in frameworks having the shifted-ribbon motif are typically rotated with their arene planes *orthogonal* to the **GS** ribbon direction, creating channels parallel to b_1. The shift of the ribbons produces a near-rectangular pillar distribution on the **GS** sheet, in contrast to the trigonal arrangement of the quasihexagonal motif. The width of the channels in the shifted-ribbon compounds, after accounting for the tilt of the pillars (ϕ), is $a_1 \cos \phi$, minus the van der Waals thickness of the pillars.

The quasihexagonal motif is generally observed when the molecular volume of a guest is near the limit of the available inclusion cavity volume of the bilayer architecture. This can be attributed to a_1 being greater than b_1, which favors inclusion of larger molecules and their attainment of commensurate structures in the channels along a_1. Unlike many other inclusion hosts, **GS** hosts rarely form incommensurate inclusion compounds. This can be directly attributed to the facile deformation of the soft **GS** host lattice and, in the case of the bilayer frameworks, the availability of two different **GS** motifs with different channel structures. Furthermore, the tendency of these materials to form commensurate structures results in stoichiometric inclusion compounds in all cases.

Greater tilting of a given pillar, i.e., larger values of ϕ, is synonymous with shorter bilayer heights and, consequently, smaller inclusion cavity volumes. Though the bilayer heights and cavity volumes generally scale with the molecular volumes of the included guests, a direct correlation is not always observed. Figure 4c,d depicts the crystal structures of two typical bilayer inclusion compounds, **G$_2$BPDS**·(*p*-dichlorobenzene) and **G$_2$BPDS**·(*p*-xylene), which both adopt the shifted ribbon **GS** sheet motif. Despite the nearly identical shapes and volumes of the two guests, the two compounds have different bilayer heights (h = 10.5 and 11.2 Å, respectively) and inclusion cavity volumes. The discrepancy implies that factors other than simple sterics can influence the structure of these inclusion compounds. Analysis of numerous inclusion compounds suggests that local ion−dipole interactions between the **G** ions, which line the floors and ceilings of the channels, and the halogen atom substituents of included guests may promote shrinkage of the bilayer height.

Despite the contributions of specific host−guest interactions, the gallery heights of **GS** inclusion compounds are inherently controllable and provide a means for systematic adjustment of intermolecular metrics between included guests. This feature is illustrated by a series of 1:1 bilayer inclusion compounds of *p*-diethynylbenzene with **G$_2$ABDS**, **G$_2$BPDS**, and **G$_2$2,6NDS** (Figure 5). In a trend that parallels the decreasing pillar lengths, the gallery heights in these inclusion compounds decrease in the order $h_{\mathbf{ABDS}}$ (12.3 Å) > $h_{\mathbf{BPDS}}$ (10.8 Å) > $h_{\mathbf{2,6NDS}}$ (9.5 Å). The *p*-diethynylbenzene guest molecules fill the host channels, aligning their arene planes nominally parallel with the channel direction. As anticipated, shrinking of the gallery height induces a corresponding increase in the tilt angle of the guest molecules, accompanied by changes in the intermolecular contacts between included guests. For example, increased guest tilting decreases the shortest distance between the centroids of the ethynyl moieties of adjacent guests, $d_{e-e,\mathbf{ABDS}}$ (5.8 Å) > $d_{e-e,\mathbf{BPDS}}$ (5.6 Å) > $d_{e-e,\mathbf{2,6NDS}}$ (5.3 Å). Systematic manipulations such as these, where intermolecular metrics may be adjusted at sub-angstrom length scales, may ultimately provide interesting opportunities for performing topochemical reactions within the confines of nanoscale inclusion cavities. Although there are numerous reports of topochemical reactions within other inclusion compounds,[22] systematic adjustment of intermolecular guest−guest metrics remains a challenge. Though the intermolecular guest−guest contacts in these compounds do not fall within topochemical criterion, and hence are unreactive, these examples illustrate the effect of metric changes in gallery height, achieved here with interchangeable pillars, on guest−guest metrics.

Architectural Isomerism and Brick Host Frameworks

Certain sterically demanding pillars, such as **1,5NDS**, that project a large "footprint" on the **GS** sheet are not capable of forming a bilayer framework. Instead, **G$_2$1,5NDS** inclusion compounds only crystallize in the simple brick architecture with one-dimensional channels filled by linear guest molecules with small cross sections (e.g., hexanenitrile). Most pillars, however, are not subject to

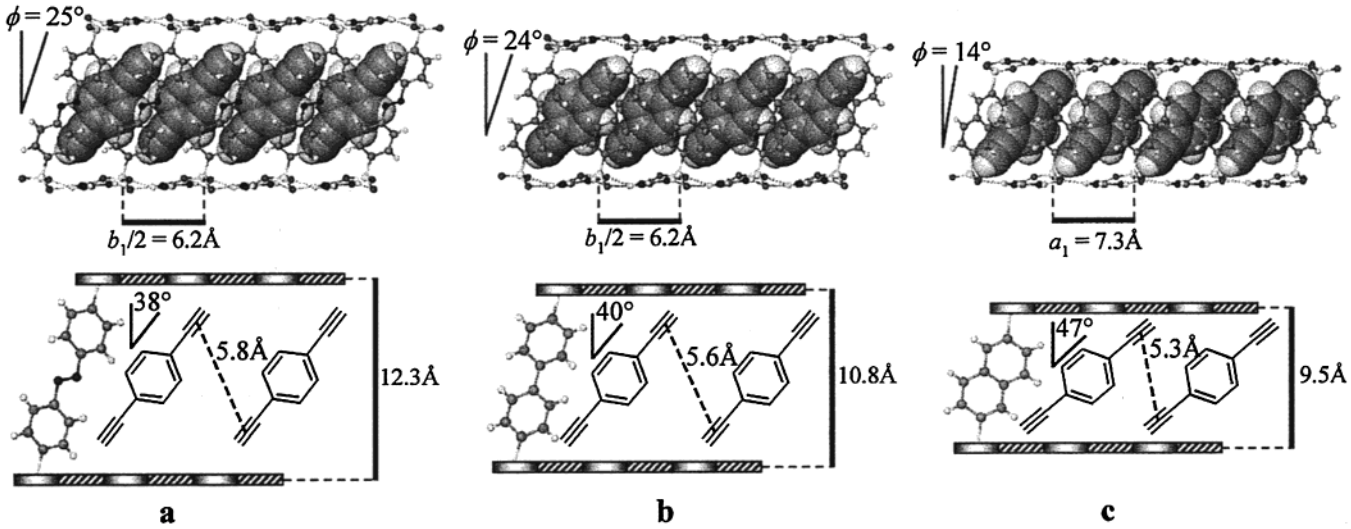

FIGURE 5. Crystal structures of (a) **G$_2$ABDS·**(*p*-diethynylbenzene), (b) **G$_2$BPDS·**(*p*-diethynylbenzene), and (c) **G$_2$2,6NDS·**(*p*-diethynylbenzene). The gallery heights, distances between centroids of the ethynyl moieties, and guest tilt angles are depicted.

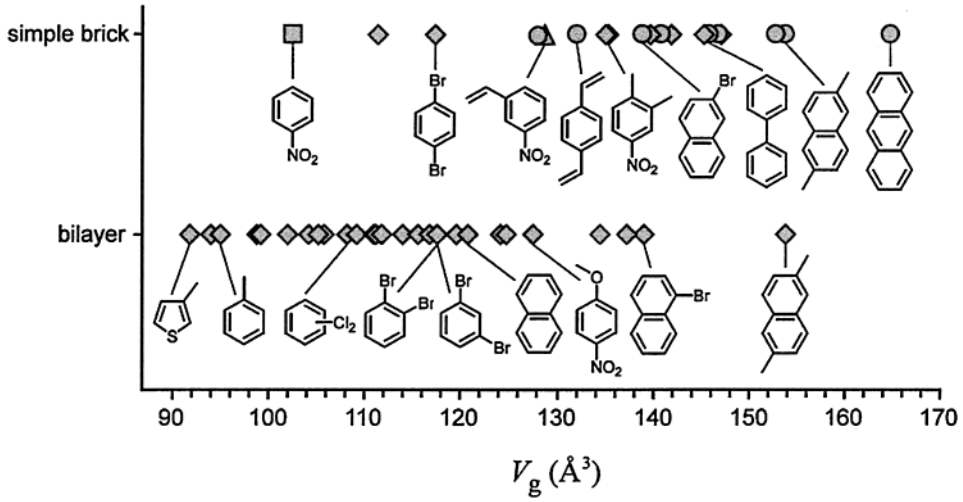

FIGURE 6. Comparison of the molecular volumes of numerous guests (V_g) with the observed architectural isomer in the **G$_2$BPDS·***n*(guest) system of inclusion compounds, revealing that smaller guests tend to promote the formation of the bilayer framework whereas larger guests template the brick isomer. Some representative guests are labeled. The diamonds (◆), circles (●), and squares (■) represent inclusion compounds with 1:1, 1:3, and 1:4 host:guest stoichiometries, respectively.

such steric constraints and can form either framework. We first demonstrated a bilayer-to-brick architectural isomerism for inclusion compounds with the **G$_2$BPDS** framework wherein the brick isomer was generated by guests or guest aggregates that were too large to fit into the inclusion cavities of the bilayer framework.[19] This isomerism, which has now been demonstrated for several other frameworks prepared from our pillar library, demonstrates that the guests serve as templates that direct the assembly of the host framework. This behavior is reminiscent of the templated synthesis of open framework zeolites and silicates by surfactant microstructures and organic imprinting molecules.[23,24] We stress that bilayer and brick frameworks generated from the same pillar are *true* isomers, with identical chemical compositions.

Examination of an extensive collection of bilayer and simple brick isomers (Figure 6) of **G$_2$BPDS·***n*(guest) inclusion compounds reveals a preference for the more open brick form with increasing guest volume (V_g), although there is no well-defined threshold for the isomer selectivity. This can attributed to (i) the inclusion of multiple small guests by the brick framework (e.g., 4 equiv of nitrobenzene), (ii) the ability of the brick framework to pucker more extensively, enabling it to shrink about guests that appear to be small enough to fit in the bilayer form (e.g., 1 equiv of *p*-dibromobenzene), (iii) specific host−guest interactions that can be optimized in a particular framework (e.g., ion−dipole host−guest interactions in **G$_2$BPDS·**(*p*-dibromobenzene) brick compound), and (iv) the ability of the bilayer framework to accommodate certain large guest molecules through deformation of the pillars (e.g., **G$_2$BPDS·**(2,6-dimethylnaphthalene), in which the **BPDS** pillars are bowed). The role of (ii) and (iii) is evident from the structures of **G$_2$BPDS·**(*o*-dibromobenzene), **G$_2$BPDS·**(*m*-dibromobenzene), and **G$_2$BPDS·**(*p*-dibromobenzene). Though the molecular volumes of the three different

guests are essentially identical, the former two promote crystallization of the bilayer framework, while the latter is included in a highly puckered brick framework with identifiable ion−dipole host−guest contacts.

Though the number of examples is not yet as large, we have confirmed that the concept of architectural isomerism is quite general, appearing also in **G_2BDS**, **$G_2$2,6NDS**, and **G_2ADS** hosts. Comparison of the four different hosts demonstrates clearly that selectivity is generally governed by the relative sizes of the pillar and guest. For example, **$G_2$2,6NDS** forms 1:1 bilayer inclusion compounds with benzene, but the **G_2BDS** host framework, with a shorter pillar, adopts the more open brick architecture in order to accommodate the same guest, albeit with a 1:3 host:guest stoichiometry. Similarly, *p*-divinylbenzene templates the formation of a brick architecture as **G_2BPDS**·3(*p*-divinylbenzene), but increasing the pillar length by using **G_2ABDS**·(*p*-divinylbenzene) results in reversion to a bilayer structure.[25]

The larger separation between pillars in the simple brick framework permits more extensive puckering than in the bilayer form, leading to an impressive range of inclusion cavity volume (V_{inc}). For example, $V_{inc} = 859$ Å^3/pillar for the slightly puckered **G_2BPDS**·3(anthracene) but is only 346 Å^3/pillar for the highly puckered **G_2BPDS**·(3-nitrostyrene). The brick host framework can also adapt to differently sized and shaped guests through turnstile rotation of the pillars about the C−S bonds. When combined with the puckering capacity of the **GS** sheet, this endows the brick host with a remarkable degree of freedom for optimizing host−guest packing.

Whereas **GS** sheet puckering in these brick frameworks principally influences the inclusion cavity volume and the number of accompanying guests, pillar rotation governs the dimensionality of inclusion cavities. The host frameworks can be classified as three distinct conformers, illustrated here by three specific examples from the **G_2BPDS**·*n*(guest) system (Figure 7). The host framework in the 1:1 inclusion compound **G_2BPDS**·(*p*-dibromobenzene) is highly puckered about the small guest molecules. This accompanying tilting of the pillars affords an essentially solid wall of biphenyl residues, flanking channels that run along b_1 (perpendicular to the **GS** ribbons). These channels, with widths equal to a_1 (minus the van der Waals width of the pillars), are occupied by guest molecules nestled in the host pockets created by the puckering. The inclusion cavity volume in this highly shrunken host is only slightly larger than that of the **G_2BPDS** bilayer framework.

Conversely, if the pillars are rotated such that their arene planes align *parallel* to the ribbon direction, as in **G_2BPDS**·4(nitrobenzene), the gallery contains 1-D channels along a_1, with width b_1 (minus the van der Waals width of the pillars), flanked by a solid wall of pillars. Intermediate degrees of pillar rotation, as observed in **G_2BPDS**·3(*p*-divinylbenzene), afford 2-D continuous inclusion cavities within the galleries. These conformers differ substantially with respect to available inclusion cavity volume, as evidenced by the different number of included molecules. The inclusion cavities of the less puckered versions actually account for approximately 70% of the total unit cell! Similar conformers have been observed for other **GS** hosts.

Interdependencies of Structural Metrics

With few exceptions, crystal engineering strategies for the synthesis of low-density inclusion frameworks have focused on the design and synthesis of solid-state architectures rather than lattice metrics. The ability to interchange the pillars of the **GS** host frameworks allows adjustment of specific structural features, such as the gallery heights of the bilayer and brick frameworks, with a facility that is rather unusual in crystal engineering. Furthermore, the family of simple brick frameworks display *metric interdependences* among specific structural features that reveal a common, well-behaved mechanism through which the host molds to differently sized and shaped guests. The generality of this mechanism and its characterization provides a route to a priori determination of key metric parameters, such as the maximum available inclusion cavity volume and lattice constants, that can guide the design and synthesis of these materials.

The lattice constant within the **GS** ribbon, a_1, is not influenced by puckering. The lattice parameter b_1, however, depends on θ_{IR} according to eq 1, where w is the fixed width (6.5 Å) of the **GS** ribbon. According to eq 1, b_1

$$b_1 = 2w \sin(\theta_{IR}/2)\ \text{Å} = 13.0 \sin(\theta_{IR}/2)\ \text{Å} \qquad (1)$$

$= 2w = 13.0$ Å in the limit of a flat sheet. For convenience and accuracy, we measure θ_{IR} from the crystal structures using discrete sulfur atoms on adjacent ribbons.[5] Equation 1, however, holds rigorously only when θ_{IR} is defined by the intersection, at the ribbon edges, of the *mean planes* of two adjacent ribbons (θ_{IR}^{actual}). Figure 8 illustrates that the measured b_1 values conform to eq 1 for their respective measured θ_{IR} values when the sheets are slightly puckered (large θ_{IR}) but diverge with increased puckering. This apparent discrepancy is due to simple geometric factors; specifically, measured θ_{IR} values become greater than θ_{IR}^{actual} with increased puckering because the sulfur atoms are displaced slightly from the ribbon edges where puckering actually occurs. The geometric correspondence between the two angles can be described by a transformed version of eq 1, which fits the observed values of b_1 over the entire range to within 4% of the experimental values.[26] The relationship between b_1 and θ_{IR} in the homologous continuously interdigitated structures observed in many guanidinium organo*mono*sulfonates also conforms to this function.

Related mathematical expressions describe the dependence of the unit cell and inclusion volumes on pillar length (l), θ_{IR}, and ϕ. An *idealized* orthorhombic **GS** brick framework is described by the lattice constants of the **GS** sheet (a_1 and b_1; $\gamma_1 = 90°$) and the bilamellar spacing c_1, according to eq 2. Tilting of the pillars ($\phi > 0$) in the highly puckered frameworks decreases c_1, but the pillars in less

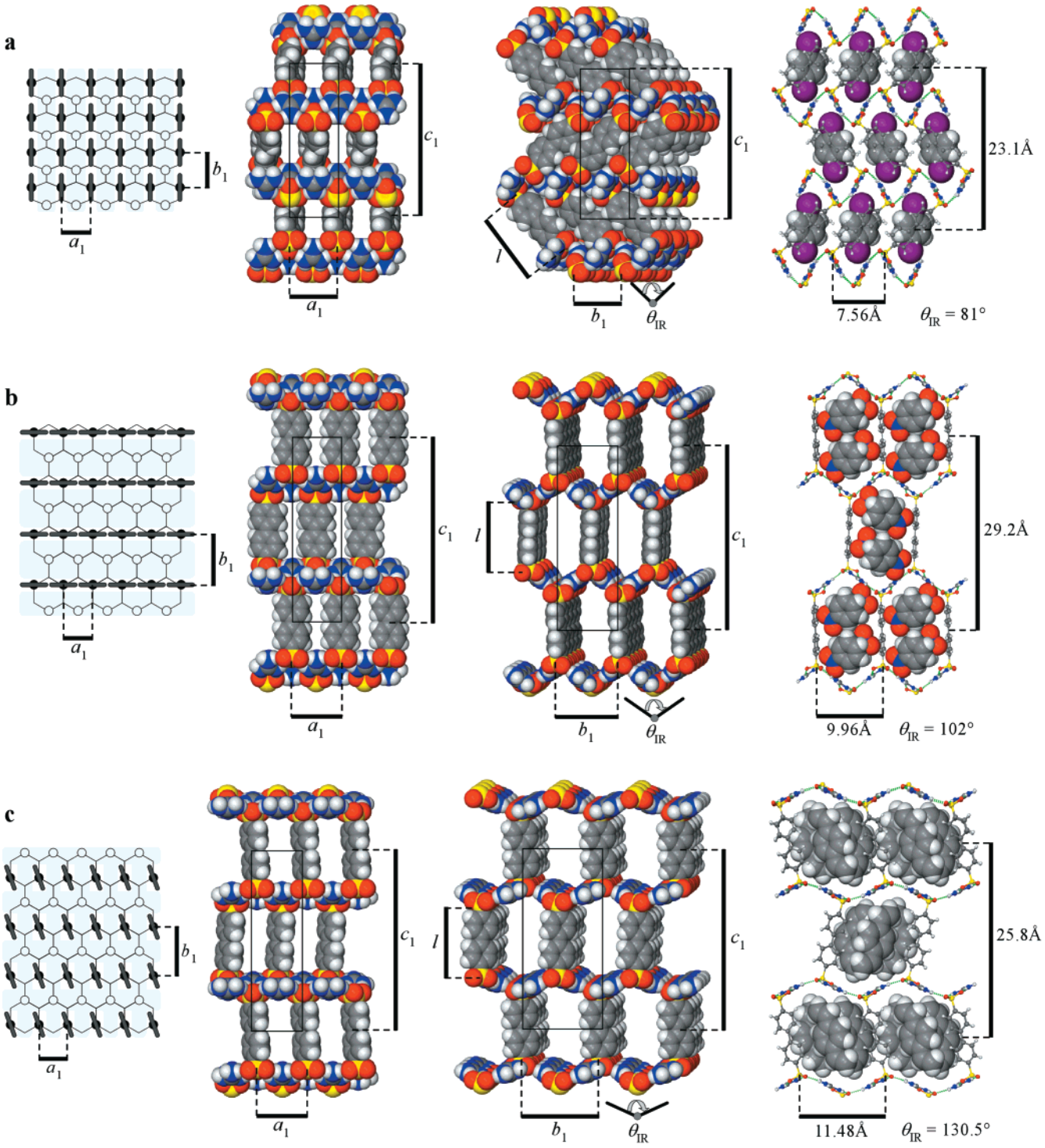

FIGURE 7. Conformational flexibility of the brick host architecture leads to three distinct conformers. (a) **G_2BPDS**·(*p*-dibromobenzene): Highly puckered **GS** sheets, with pillars aligned along b_1, orthogonal to the ribbon direction, produce 1-D channels, flanked by the pillars, of width a_1. (b) **G_2BPDS**·4(nitrobenzene): Less puckered sheets afford galleries wherein the pillars align along a_1, parallel to the ribbon direction, to produce 1-D channels of width b_1. (c) **G_2BPDS**·3(1,4-divinylbenzene): Less puckered sheets can also afford galleries wherein the pillar rotation is intermediate between (a) and (b), generating a 2-D continuous guest network with the guests surrounding the pillars. The schematic illustrations at the left depict a top view of the gallery regions for each case. The guest-filled channels are shaded and the aromatic planes of the **BPDS** pillars are depicted as black rectangles.

puckered brick frameworks are essentially normal to the **GS** sheet ($\phi \approx 0°$), so that c_1 depends only on θ_{IR} and l. The first term in eq 2 describes the increase in the effective thickness, t, of the **GS** sheets with puckering, which increases c_1. The second term describes the contribution from the pillar length and tilt. Equations 1 and 2 can be combined to give eq 3, which provides the metric relationship between unit cell volume (V_{cell}) and θ_{IR}.

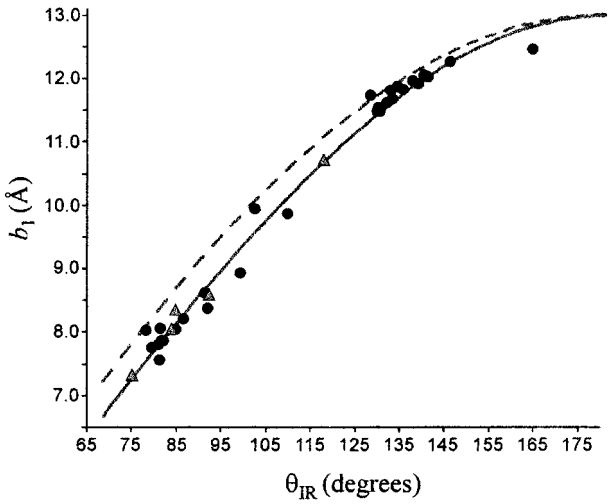

FIGURE 8. Plot of observed b_1 lattice parameters as a function of the observed θ_{IR} values for [**G**][organomonosulfonate] compounds with the continuously interdigitated architecture (△) and [**G**]$_2$-[organodisulfonate] compounds with the simple brick framework (●), which both exhibit the same pillar topology. The lines represent eq 1 (- - -) and its transformed version (—).[26]

$$c_1 = 13.0 \cos(\theta_{IR}/2) + 2l \cos \phi \text{ Å} \quad (2)$$

$$V_{cell} = a_1 b_1 c_1 = [7.5][13.0 \sin(\theta_{IR}/2)][13.0 \cos(\theta_{IR}/2) + 2l \cos \phi] \text{ Å}^3 \quad (3)$$

The maximum inclusion cavity volume (V_{inc}^{max}), which is governed by the maximum unit cell volume (V_{cell}^{max}), for a selected **GS** host framework establishes the size limit for commensurate guest inclusion. Though one might assume that V_{cell}^{max} and V_{inc}^{max} are achieved at the maximum b_1 value, where the **GS** sheet is flat and the pillars are at their maximum separation along b$_1$, the product b_1c_1 is not maximal for a flat sheet (a_1 is constant). Though puckering shortens b_1, it is accompanied by an increase in t and c_1, as well as the formation of canopies at the floor and ceiling of each gallery that can increase the volume of the inclusion cavity (Figure 9). The puckering angle at which V_{cell}^{max} and V_{inc}^{max} are achieved can be determined for a given pillar from the first derivative of eq 3 with respect to θ_{IR}, solving for $dV_{cell}/d\theta_{IR} = 0$. Because eq 3 depends on l, V_{cell}^{max} is affected by the length of the pillar used to construct the framework. The dependence of V_{cell} on θ_{IR} according to eq 3 is graphically represented in Figure 9 by "master curves" for selected pillars, along with experimental values available at the time of this writing. The V_{inc} values can be calculated directly from $V_{inc} = V_{cell} - 2V_{host}$ (the factor of 2 is required by the stoichiometry of the unit cell).

Good agreement between the experimental (θ_{IR},V_{cell}) values for the slightly puckered brick inclusion compounds and those expected from eq 3 is evident in Figure 9. Interestingly, the experimentally observed values of V_{cell} = 2383 Å^3 and θ_{IR} = 128° for **G$_2$BPDS**·3(anthracene), which has the largest unit cell volume yet observed for the **G$_2$BPDS** framework, compare favorably with the calculated values of V_{cell}^{max} = 2359 Å^3 and $\theta_{IR}@V_{cell}^{max}$ = 132°. The well-behaved interdependence of these metric parameters signifies a universal mode of structural adaptation of the flexible host lattice in which its components (i.e., sheets, ribbons, pillars) adjust synchronously to optimize host−guest packing. These examples illustrate that crystal *metrics*, a vital component of crystal engineering, can be surmised reliably if the conformational behavior of a given crystal architecture is fully elucidated and well-behaved. Though the simple brick framework has not yet been observed for all the pillars in our library, the values of V_{inc}^{max} can be anticipated, a priori, from the master curves by $V_{inc}^{max} = V_{cell}^{max} - 2V_{host}$. This represents the upper limit for the inclusion cavity volume in the frameworks for each pillar. After accounting for a packing fraction typical for molecular crystals (ca. 0.7), these values can be used to select guests to fit in a particular host framework or, conversely, to select a host framework to accommodate a particular guest molecule. These master curves thus provide quantitative guidance for the design of these materials.

Metric Engineering through Structural Mimicry

One of the principal goals of crystal engineering is the prediction of crystal packing based on known structures, or structural motifs, in existing materials. Though crystal engineering has been modestly successful with respect to replicating general solid-state features, few examples exist wherein the lattice metrics can be predicted from known structures. We recently demonstrated that this can be achieved in certain cases wherein the pillars and guests are isostructural, as in **G$_2$NDS**·3(naphthalene), **G$_2$BPDS**·3(biphenyl), and **G$_2$ADS**·3(anthracene).[27] Remarkably, the guests and their isostructural pillars are organized between the **GS** sheets in a herringbone motif that is essentially *identical* to the herringbone layer motif observed in the crystal structures of the respective pure guests, with the organodisulfonate pillars substituting for every fourth molecule in the herringbone motif of the pure guests (Figure 10).

The metrics of these herringbone pillar−guest ensembles can be described by their in-plane lattice dimensions, a_1 and b_1, the latter varying with the degree of puckering required by the host to achieve an innate pillar−guest packing. Though the stiffness of the **GS** ribbons along the ribbon direction prevents a_1 from conforming exactly with the corresponding lattice parameter in the respective pure guests (a_G), the 7.5 Å repeat distance along the **GS** ribbon is within 8% of the guest-only values. This mismatch is compensated by the ability of the framework to compress, by puckering, along b$_1$, so that the values of b_1 are nearly identical to $2b_G$, the corresponding lattice parameter in the pure guest crystals (Table 1). Furthermore, the average arene−arene dihedral angles (δ) are essentially identical to the values in the respective pure guests.

The θ_{IR} values for these compounds can be predicted, using eq 1, substituting the *guest-only* values of $2b_G$ for b_1. This affords $\theta_{IR,calc}$ values that compare favorably to

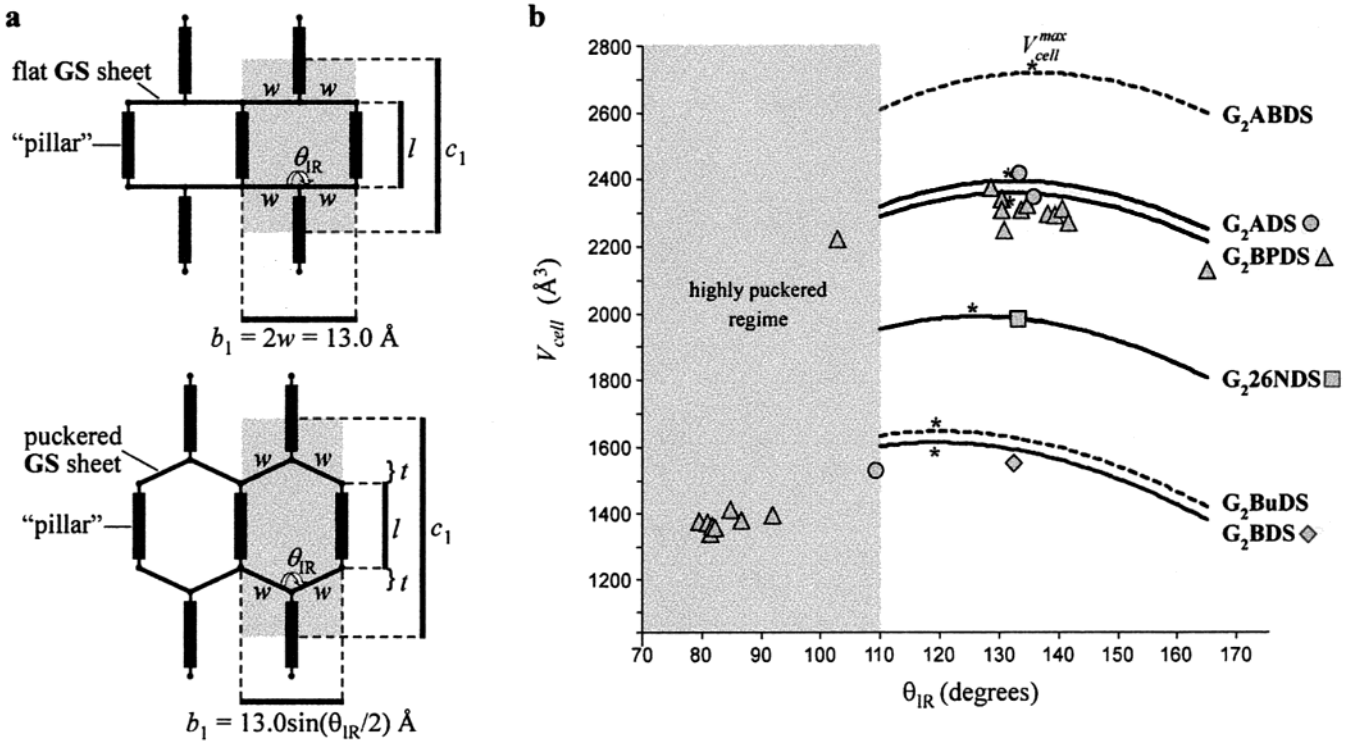

FIGURE 9. (a) Schematic representation of an unpuckered and a slightly puckered brick framework, illustrating the change in V_{cell} and V_{inc} with θ_{IR}. (b) V_{cell} vs θ_{IR} measured for various simple brick inclusion compounds (circles, triangles, squares, and diamonds). The dependence of V_{cell} on θ_{IR}, according to eq 3 with $\phi = 0°$, is depicted by the solid and dashed lines. The dashed lines correspond to frameworks that have not yet been observed in the brick architecture. The asterisk indicates the expected value of V_{cell}^{max} and the value of θ_{IR} for V_{cell}^{max} and V_{inc}^{max}. The values of V_{cell} for the highly puckered **G$_2$BPDS** frameworks are depicted at the lower left in the highly puckered regime. These values conform to eq 3 if the measured value of ϕ in each case is included.

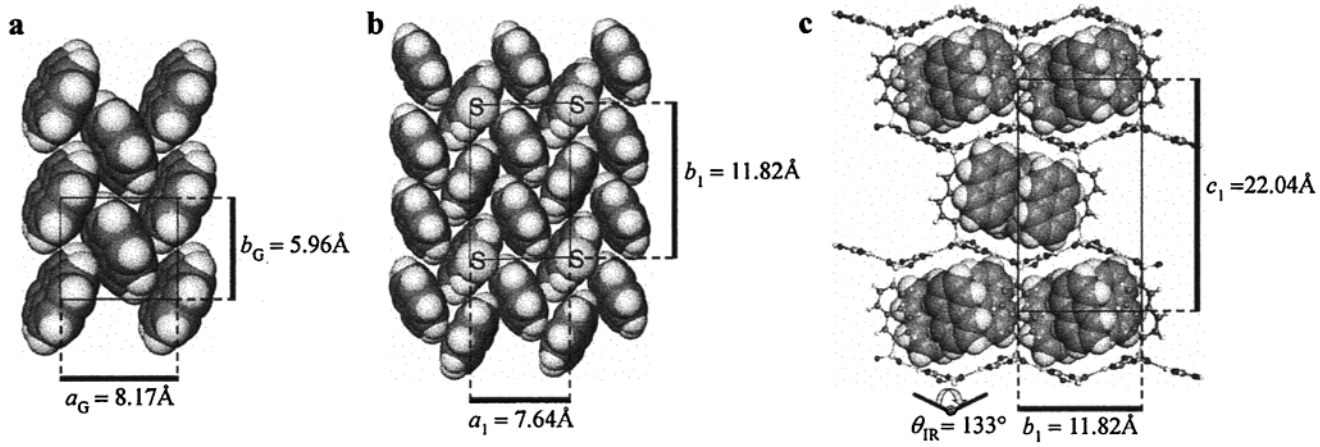

FIGURE 10. (a) Herringbone motif in the *ab* plane of pure naphthalene. (b) The herringbone pillar−guest packing in the *ab* plane of the simple brick inclusion compound **G$_2$NDS**·3(naphthalene). The **G** ions and sulfonate oxygen atoms of the upper **GS** sheet have been removed to allow viewing of the pillar−guest ensembles. The pillars can be identified by the labeled sulfur atoms. (c) **G$_2$NDS**·3(naphthalene) as viewed down the **GS** ribbons that run along the a_1 axis.

$\theta_{IR,obs}$, as measured from the crystal structures (Table 1). The predicted bilamellar spacings, c_1, calculated with eq 3 using $\theta_{IR,calc}$ and l (assuming $\phi = 0$), also agree with the observed values of c_1.

The agreement between the metric parameters of the inclusion compounds and their corresponding values in the pure guest structures demonstrates that the *major driving force for pillar−guest organization in the inclusion compounds is the achievement of an innate herringbone motif that mimics molecular organization in the pure guests.* The achievement of herringbone pillar−guest motifs that mimic the molecular packing in the crystal structures of the guests alone is made possible by the soft H-bonded **GS** sheets and the freely rotating isostructural pillars.

Interestingly, the inclusion compound **G$_2$BDS**·3(benzene), which also has isostructural pillars and guests, exhibits herringbone pillar−guest packing that approaches

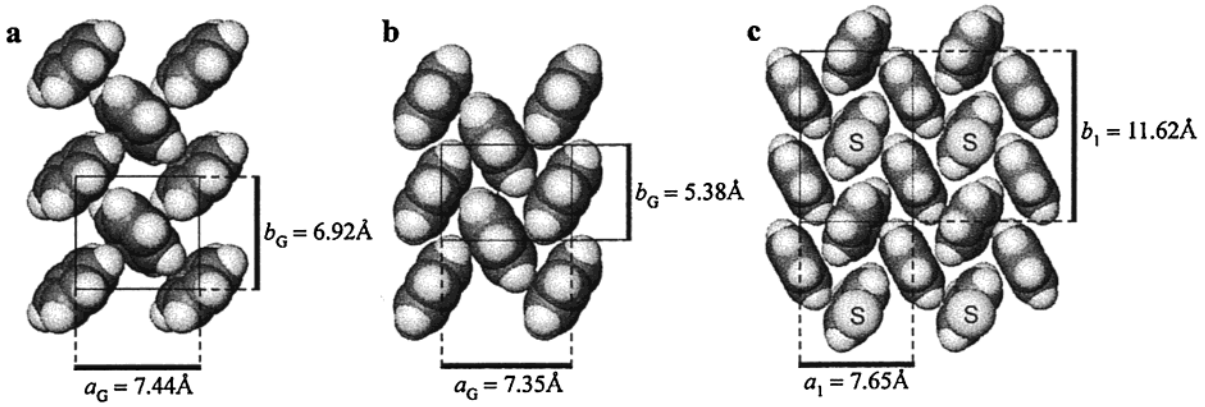

FIGURE 11. (a) Top view of the herringbone packing of ambient pressure form of benzene. (b) Top view of the herringbone packing of the high-pressure form of benzene. (c) Top view of the herringbone packing of the pillar/guest ensembles in the simple brick inclusion compound **G_2BDS**·3benzene. The **G** ions and sulfonate oxygen atoms of the upper **GS** sheet have been removed to allow viewing of the pillar−guest ensembles. The pillars can be identified by the labeled sulfur atoms.

Table 1. Comparison of Structural Parameters of GS Inclusion Compounds and Pure Guest Structures

compound	$b_{1,obs}$ and a_G (Å)	$b_{2,obs}$ and $2b_G$ (Å)	$\theta_{IR,obs}$ (deg)	$\theta_{IR,calc}$ (deg)	$c_{1,obs}$ (Å)	$c_{1,calc}$ (Å)	δ (deg)
1	$b_1 = 7.64$	$b_2 = 11.82$	133	133	22.04	22.2	54
naphthalene	$a_G = 8.17$	$2b_N = 11.92$					52
2	$b_1 = 7.66$	$b_2 = 11.49$	130	120	26.31	27.7	61
biphenyl	$a_B = 8.12$	$2b_B = 11.28$					67
3	$b_1 = 7.56$	$b_2 = 11.96$	133	135	26.85	26.6	50
anthracene	$a_A = 8.47$	$2b_A = 12.00$					51

the high-pressure form of solid benzene (Figure 11). The areal density of the herringbone layers in the ambient pressure form is 3.89 molecules nm^{-2}, compared to 5.06 and 4.50 molecules nm^{-2} for the high-pressure form of benzene and the pillar−guest layers of **G_2BDS**·3(benzene), respectively. Notably, the **GS** host cannot accommodate the ambient packing density because $2b_G$ for pure benzene under ambient conditions is 13.84 Å, which exceeds the 13 Å limit for b_1. The **GS** host effectively exerts a lattice pressure that enforces a packing of benzene pillars and guest under ambient conditions that more closely resembles the high-pressure form.

Epilogue

The versatility and reliability of the **GS** host system, which is a direct consequence of its conformational softness and ability to adapt to differently sized and shaped guest molecules, have prompted several new research efforts in our laboratory. We have demonstrated that **GS** frameworks can promote polar ordering of guest molecules even if the host itself is not inherently polar,[28] but recently we have synthesized inherently polar **GS** host frameworks that enforce polar guest alignment. During exploration of the guest templating phenomenon, we have also discovered several new architectural isomers that are variants of the continuous simple brick form but have different inclusion cavity shapes. The observation of these new isomers reveals a universality for the **GS** host system that is greater than we had originally anticipated. The flexibility of the **GS** sheet has also allowed us to synthesize crystalline materials in which the sheets "curl", instead of pucker, into open-ended tubes of various diameters, heralding a new class of rigid nanotubes that resemble rodlike surfactant microstructures. We have also demonstrated crystallization-based separations of isomeric guests using **GS** host frameworks based on reversible assembly and disassembly of the inclusion compounds under mild conditions. These materials may have distinct advantages over more traditional zeolitic materials for the separations of fine chemicals, as crystallization of the inclusion compounds is not limited by diffusion of the guest molecules in to and out of pre-existing pores. Furthermore, guest inclusion is stoichiometric with very high mass efficiency. We anticipate that further investigation of these materials and the principles governing their formation will advance the understanding of crystal engineering and produce a new generation of designer materials based on supramolecular assembly.

The authors are grateful for support from the National Science Foundation (DMR-9908343) and the University of Minnesota Materials Research Science and Engineering Center (DMR-9809364). K.T.H. is grateful for a postdoctoral fellowship from the Natural Sciences and Engineering Research Council of Canada.

References

(1) (a) Schmidt, G. M. J. Photodimerization in the solid-state. *Pure Appl. Chem.* **1971**, *27*, 647−678. (b) Desiraju, G. R. *Crystal engineering: The design of organic solids*; Elsevier: New York, 1989.

(2) For an introduction to organic inclusion compounds, see: (a) Molecular inclusion and molecular recognition. Clathrates I and II. *Topics in Current Chemistry*; Weber, E., Ed.; Springer-Verlag: New York, 1987 and 1988; Vols. 140 and 149. (b) *Comprehensive Supramolecular Chemistry*; Atwood, J. A., Davies, J. E. D., NacNicol, D. D., Vögtle, F., Lehn, J.-M., Eds.; Elsevier Science: New York, 1996; Vol. 6. (c) *Inclusion Compounds. Structural aspects of inclusion compounds formed by organic host lattices*; Atwood, J. A., Davies, J. E. D., MacNicol, D. D., Eds.; Academic: London, 1984; Vol. 2.

(3) Li, H.; Eddaoudi, M.; O'Keeffe, M.; Yaghi, O. M. Design and synthesis of an exceptionally stable and highly porous metal-organic framework. *Nature* **1999**, *402*, 276−279.
(4) Langley, P. J.; Rawson, J. M.; Smith, J. N. B.; Schuler, M.; Bachmann, R.; Schweiger, A.; Palacio, F.; Antorrena, G.; Geschheidt, G.; Quintel, A.; Rechsteiner, P.; Hulliger, J. Probing magnetic exchange interactions in molecular magnets: an inclusion compounds of a dithiadiazolyl radical. *J. Mater. Chem.* **1999**, *9*, 1431−1434.
(5) Brown, M. E.; Hollingsworth, M. D. Stress-induced domain reorientation in urea inclusion compounds. *Nature* **1995**, *376*, 323−327.
(6) Ramamurthy, V.; Eaton, D. F. Perspectives on solid-state host−guest assemblies. *Chem. Mater.* **1994**, *6*, 1128−1136.
(7) Toda, F.; Hyoda, S.; Okada, K.; Hirotsu, K. Isolation of anhydrous hydrazine as stable inclusion complexes with hydroquinone and *p*-methoxyphenol, and their solid-state reaction with esters which gives pure hydrazides. *J. Chem. Soc., Chem. Commun.* **1995**, 1531−1532.
(8) Endo, K.; Koike, T.; Sawaki, T.; Hayashida, O.; Masuda, H.; Aoyama, Y. Catalysis by organic solids. Stereoselective Diels−Alder reactions promoted by microporous molecular crystals having an extensive hydrogen-bonded network. *J. Am. Chem. Soc.* **1997**, *119*, 4117−4122.
(9) Hirsch, K. A.; Wilson, S. R.; Moore, J. S. A Packing Model for Interpenetrated Diamondoid Structures—An Interpretation Based on the Constructive Interference of Supramolecular Networks. *Chem. Eur. J.* **1997**, *3*, 765−771.
(10) Reineke, T. M.; Eddaoudi, M.; Moler, D.; O'Keeffe, M.; Yaghi, O. M. Large Free Volume in Maximally Interpenetrating Networks: The Role of Secondary Building Units Exemplified by $Tb_2(ADB)_3[(CH_3)_2SO]_4{\cdot}16[(CH_3)_2SO]$. *J. Am. Chem. Soc.* **2000**, *122*, 4843−4844.
(11) Subramanian, S.; Zaworotko, M. J. Porous solids by design: $[Zn(4,4'\text{-bpy})_2(SiF_6)]_n{\cdot}x$DMF, a single framework octahedral coordination polymer with large square channels. *Angew. Chem., Int. Ed. Engl.* **1995**, *34*, 2129−2129.
(12) Russell, V. A.; Etter, M. C.; Ward, M. D. Layered materials by molecular design: structural enforcement by hydrogen bonding in guanidinium alkane- and arenesulfonates. *J. Am. Chem. Soc.* **1994**, *116*, 1941−1952.
(13) Russell, V. A.; Etter, M. C.; Ward, M. D. Guanidinium *para*-substituted benzenesulfonates: competitive hydrogen bonding in layered structures and the design of nonlinear optical materials. *Chem. Mater.* **1994**, *6*, 1206−1217.
(14) Russell, V. A.; Ward, M. D. Two-dimensional hydrogen-bonded assemblies: the influence of sterics and competitive hydrogen bonding on the structures of guanidinium arenesulfonate networks. *J. Mater. Chem.* **1997**, *7*, 1123−1133.
(15) The θ_{IR} values reported in our earlier papers were obtained only through estimates, obtained graphically, of θ_{IR}^{actual}, the puckering defined by intersecting adjacent ribbons. We have since found that measurement of θ_{IR} from discrete sulfur atom positions is more convenient and reliable for metric analysis of **GS** compounds. In the case of flat bilayer sheets, $\theta_{IR} = \theta_{IR}^{actual} = 180°$, but $\theta_{IR} = 165°$ for flat sheets in the simple brick isomer because the sulfur atoms that define puckering alternate their positions on opposite sides of a sheet.
(16) Batten, S.; Robson, R. Interpenetrating nets: ordered, periodic entanglement. *Angew. Chem., Int. Ed.* **1998**, *37*, 1461−1494.
(17) Architectural isomerism is a subclass of supramolecular isomerism, which also includes frameworks having identical compositions but different supramolecular connectivity (e.g., **GS** hosts with the same pillar but different **GS** H-bonding motifs).
(18) Russell, V. A.; Evans, C. C.; Li, W.; Ward, M. D. Nanoporous molecular sandwiches: pillared two-dimensional hydrogen bonded networks with adjustable porosity. *Science* **1997**, *276*, 575−579.
(19) Swift, J. A.; Pivovar, A. M.; Reynolds, A. M.; Ward, M. D. Template-directed architectural isomerism of open molecular frameworks: engineering of crystalline clathrates. *J. Am. Chem. Soc.* **1998**, *120*, 5887−5894.
(20) Swift, J. A.; Reynolds, A. M.; Ward, M. D. Cooperative host−guest recognition in crystalline clathrates: steric guest ordering by molecular gears. *Chem. Mater.* **1998**, *10*, 4159−4168.
(21) The volume of any **GS** host framework (V_{host}) can be estimated a priori, by $V_{host} = V_{org} + 189$ Å^3, where V_{org} is the volume of the parent organic molecule from which the organodisulfonate pillar is derived, as determined from Connolly surfaces, using a probe radius of zero and a dot density of 100/Å^2 (MSI Cerius^2, v 3.5). The 189 Å^3 term accounts for the substitution of two terminal hydrogen atoms with sulfonate residues and **G** ions in the typical H-bonded arrangement. This term was determined by subtracting the inclusion cavity volume, V_{inc}, also determined from the total volume of the unit cell, V_{cell}, for numerous **GS** inclusion compounds. V_{inc} was calculated using "fine" grid spacing and a probe radius of 0.5 Å. Our values of V_{org} tend to be systematically lower, by up to ca. 5%, than the corresponding reported values: Kitaigorodsky, A. I. *Molecular Crystals and Molecules*; Academic Press: New York, 1973.
(22) Tanaka, K.; Toda, F. Solvent-Free Organic Synthesis. *Chem. Rev.* **2000**, *100*, 1025−1074.
(23) Davis, M. E.; Katz, A.; Ahmad, W. R. Rational catalyst design via imprinted nanostructured materials. *Chem. Mater.* **1996**, *8*, 1820−1839.
(24) Huo, Q.; Margolese, D. I.; Stucky, G. D. Surfactant control of phases in the synthesis of mesoporous silica-based materials. *Chem. Mater.* **1996**, *8*, 1147−1160.
(25) Evans, C. C.; Sukarto, L.; Ward, M. D. Sterically controlled architectural reversion in hydrogen-bonded crystalline clathrates. *J. Am. Chem. Soc.* **1999**, *121*, 320−325.
(26) The function relating b_1 and θ_{IR} in eq 1 rigorously applies to θ_{IR}^{actual}. To compare the measured θ_{IR} values with expected ones, a transformed version of eq 1 must be used wherein θ_{IR} is described by

$$\theta_{IR} = 2\tan^{-1}\left[\frac{13.0\sin(\theta_{IR}^{actual}/2)}{13.0\cos(\theta_{IR}^{actual}/2) - 2y\cos(\theta_{IR}^{actual}/2)}\right]$$

where y accounts for the displacement of the sulfur positions from the long edge of the **GS** ribbon. The data indicate a best fit to $y \approx 0.4$ Å, which is comparable to the value expected from inspection of the ribbons.
(27) Holman, K. T.; Ward, M. D. Metric engineering of crystalline inclusion compounds by structural mimicry. *Angew. Chem., Int. Ed.* **2000**, *39*, 1653−1656.
(28) Swift, J. A.; Ward, M. D. Cooperative polar ordering of accentric guest molecules in topologically controlled host frameworks. *Chem. Mater.* **2000**, *12*, 1501−1504.

AR970272F